Erasmus University Rotterdam
Erasmus School of Economics

Estimation and forecasting of left-tail risk measures with an application to cryptocurrencies

Bachelor Thesis Econometrics and Operations research,
Quantitative Finance

Name student: Fleur kelders
Student ID number: 497708
Supervisor: Prof. dr. Chen Zhou
Second assessor: Bram van Os

Date final version: 4/7/2021

Abstract

Cryptocurrencies have become more and more popular of the last years. They can be responsible for large returns, however this comes at a cost of large volatility and therefore brings more risk. This paper constructs forecasts for the conditional Value-at-Risk (CVaR) and conditional expected shortfall (CES) measures. In a simulation study, the performance of the Hill estimator versus the performance of the MR estimator is examined. Also the use of a data-dependent choice of upper order statistics used in the methodology is investigated. An application to stock indices and cryptocurrency prove that the MR estimator which seems to improve forecasts in the simulation study, does not work well with empirical data.

Contents

List of Figures

List of Tables

1 Introduction

Modeling risk and volatility of assets is a highly researched topic in econometrics and economics as investors are always concerned about the risk-and-return trade-off in their portfolios. Especially downside risk is of interest as downside risk implies losses which are less preferred than positive extreme returns. Therefore, research has been done in modeling tail risk measures. Which are relevant measures for estimating the risk. Cryptocurrencies form an asset class that is known for their extreme volatility. They have gained a lot of popularity over the last five years leading to a total global market capitalization of over 2.2 trillion USD, with Bitcoin (BTC) being the largest cryptocurrency with a market capitalization of 1.08 trillion USD. Cryptocurrencies are known to have possible high returns, high volatility, large skewness, and extreme kurtosis (Zhang et al., 2018). This makes the modeling of risk of cryptocurrencies even more challenging.

To model time series of financial returns, ARMA-GARCH models are often used. Hoga (2019) shows that they have overall good performance in estimating conditional tail risk measures. Popular risk measures are Value-at-Risk (VaR) and expected shortfall (ES) which are also widely used to measure (downside) risk.

In this paper, I investigate the performance of these conditional tail risk measures as applied to cryptocurrency data. Conditional Value-at-Risk is by Hoga (2019) defined as follows: 'the loss that is exceeded only with some small probability given the history of past returns', where the conditional shortfall is referred to as: 'the expected loss beyond CVaR conditional on past returns'. I investigate some methods using extreme value theory (EVT) in constructing confidence intervals for the tail risk measures. I formulate the following research question:

Does the moments ratio (MR) estimator for the extreme value index give better CVaR and CES predictions than the Hill estimator for cryptocurrency data?

First, I investigate whether using the moments ratio (MR) estimator of Danielsson et al. (1996) or the Hill estimator of Hill (1975) gives better results. Furthermore, I compare the benefit of using the idea of self-normalization in computing the confidence intervals as opposed to using the normal approximation. The methods are applied to different cryptocurrencies and a cryptocurrency index to examine which method gives the best CVaR and CES forecasts with corresponding confidence intervals.

1.1 Literature review

Hoga (2019) applies extreme value theory to derive extreme conditional Value-at-Risk (CVaR) and conditional expected shortfall (CES) estimates. They construct confidence intervals using the concept of self-normalization. They show that a data-dependent choice of the number of upper-order statistics included in the estimation gives better simulation results. Also, they show in the simulation study that the MR estimator is slightly more preferable than the Hill estimator when using self-normalization. The empirical application to stock market indices showed that these methods lead to improvements in the CVaR and CES forecasts.

Feng et al. (2018) investigates the extreme characteristics of seven cryptocurrencies. They found that among cryptocurrencies, the right-tail correlations are much less strong compared to the left-tail correlations. However, the left-tail correlations, as well as the cross-tail correlations, were independent with selected stock indices which suggests that cryptocurrencies can be a good diversifier for a traditional portfolio. Chuen et al. (2017) uses the Cryptocurrency Index (CRIX) to investigate the risk and return characteristics of a portfolio consisting of cryptocurrencies. They show that the risk-return performance of a traditional portfolio is improved when CRIX is added to the portfolio but the results need to be handled with care.

In this paper, I apply the methods to three cryptocurrencies and to a cryptocurrency index. To my knowledge, there has not been research into these specific measures applied to cryptocurrency. Therefore, this paper adds to the existing literature on cryptocurrencies.

According to the simulation results, the MR estimator does improve the CVaR and CES forecasts. It significantly improves the coverage of the estimated intervals, but it comes at the cost of wider intervals. Furthermore, the use of self-normalization instead of normal approximation in constructing the intervals also largely improves the coverage but again leading to larger intervals. The application to stock indices opposes this result and shows that the MR estimator does not perform well in forecasting the CVaR, but the Hill estimator does. Lastly, the application to cryptocurrency data shows that the Hill estimator performs better than the MR estimator. The data-dependent method for choosing the number of upper order statistics also proofs to be unsuitable for cryptocurrency data.

This paper proceeds as follows; in section 2, I will explain the used models and develop the estimators. In section 3 the used data is discussed and relevant statistics are presented. Section 4 shows the results of the simulation study. Then, in section 5.1 the application to stock indices is performed and in section 5.2 the application to cryptocurrencies is executed. Lastly, in section 6 the results are concluded.

2 Methodology

2.1 Model Setup

Following and using the notation of Hoga (2019), I will work with an ARMA($\bar{p}, \bar{q}$) model for the loss returns $\{X_i\}_{i\in\mathbb{Z}}$ by negating the returns of an asset. In this way, we can examine the right tail of $\{X_i\}$ and thereby examine the risk measures of the returns.

$$X_i = \sum_{j=1}^{\bar{p}} \phi_j^\circ X_{i-j} + \varepsilon_i - \sum_{j=1}^{\bar{q}} \vartheta_j^\circ \varepsilon_{i-j}. \tag{1}$$

I use a GARCH(p, q) model for the errors $\{\varepsilon_i\}_{i\in\mathbb{Z}}$,

$$\varepsilon_i = \sigma_i U_i \quad \text{with} \quad \sigma_i^2 = \omega^\circ + \sum_{j=1}^{p} \psi_j^\circ \varepsilon_{i-j}^2 + \sum_{j=1}^{q} \beta_j^\circ \sigma_{i-j}^2. \tag{2}$$

Here $\{U_i\}$ are independent and identically distributed (iid) with $E[U_1] = 0$ and $Var(U_1) = 1$. Define $\boldsymbol{\theta} = (\phi_1, \ldots, \phi_{\bar{p}}, \vartheta_1, \ldots, \vartheta_{\bar{q}}, \omega, \psi_1, \ldots, \psi_p, \beta_1, \ldots, \beta_q)^\top$ a generic parameter vector where the superscript $\circ$ is used to indicate the true unknown parameters.

These are the right-tail measures, however, for applications it makes more sense to use the left tail CVaR and CES as this is of much more interest to investors. To estimate the risks (left tail) I convert the return series to a 'loss return' series by negating the observations: $\{X_i^{neg} = -X_i\}$. In this way we can examine the right tail of the loss returns and thereby examine the risk measures of the data.

Next, I filter out the error terms for given θ:

$$\varepsilon_i(\boldsymbol{\theta}) = X_i - \sum_{j=1}^{\bar{p}} \phi_j X_{i-j} + \sum_{j=1}^{\bar{q}} \vartheta_j \varepsilon_{i-j}(\boldsymbol{\theta}), \tag{3}$$

$$\sigma_i^2(\boldsymbol{\theta}) = \omega + \sum_{j=1}^{p} \psi_j \varepsilon_{i-j}^2(\boldsymbol{\theta}) + \sum_{j=1}^{q} \beta_j \sigma_{i-j}^2(\boldsymbol{\theta}). \tag{4}$$

Here, $\varepsilon_i(\boldsymbol{\theta})$ in (3) and $\sigma_i^2(\boldsymbol{\theta})$ in (4) will be estimated later on.

2.2 Estimators

For estimation I use sample $X_1, ..., X_n$, we set $\tilde{X}_i = X_i$ for $i = 1, ..., n$. Next, we set $0 = \tilde{X}_0 = \tilde{X}_{-1} = ...$, $0 = \hat{\varepsilon}_0(\boldsymbol{\theta}) = \hat{\varepsilon}_{-1}(\boldsymbol{\theta}) = ..$ and $0 = \hat{\sigma}_0^2(\boldsymbol{\theta}) = \hat{\sigma}_{-1}^2(\boldsymbol{\theta}) = ...$. The following estimators are used for given θ:

$$\widehat{\varepsilon}_i(\boldsymbol{\theta}) = \tilde{X}_i - \sum_{j=1}^{\bar{p}} \phi_j \tilde{X}_{i-j} + \sum_{j=1}^{\bar{q}} \vartheta_j \widehat{\varepsilon}_{i-j}(\boldsymbol{\theta}), \tag{5}$$

$$\widehat{\sigma}_i^2(\boldsymbol{\theta}) = \omega + \sum_{j=1}^{p} \psi_j \widehat{\varepsilon}_{i-j}^2(\boldsymbol{\theta}) + \sum_{j=1}^{q} \beta_j \hat{\sigma}_{i-j}^2(\boldsymbol{\theta}). \tag{6}$$

Then, $\hat{U}_i$ is defined as the residual and calculated as follows: $\hat{U}_i := \widehat{\varepsilon}_i(\widehat{\theta})/\widehat{\sigma}_i(\widehat{\theta})$, where $\widehat{\theta}$ is the parameter vector with estimated coefficients.

Throughout this paper I assume that U_i has distribution function F. Hoga (2019) defines the $(1-1/x)$-quantile $U(x)$ as $U(x) := F^{\leftarrow}(1-1/x)$, where $F^{\leftarrow}$ is the left-continuous inverse of F. We assume that $U(\cdot)$ has extreme value index $\gamma > 0$. This extreme value index is a measure for the heaviness of $F^{\leftarrow}$, the index is larger for heavier right-tail. Following the procedure of Hoga (2019) we reform the ARMA-GARCH model as; $X_{n+1} = \mu_{n+1} + \sigma_{n+1} U_{n+1}$. Here, μ_{n+1} and σ_{n+1} are the estimated mean and volatility of the returns respectively.

In order to estimate the CVaR and CES, μ_{n+1} and σ_{n+1} need to be estimated first. μ_{n+1} will be estimated recursively according to:

$$\widehat{\mu}_{n+1} = \tilde{\phi}_1 X_n - \tilde{\vartheta}_1 (X_n - \widehat{\mu}_n) \tag{7}$$

$\widehat{\sigma}_{n+1}$ is estimated as the root of equation (6). Thereafter, the VaR ($(1-\alpha)$-quantile) and the expected shortfall of U_i need to be estimated. These are defined as $\hat{x}_\alpha^U$ and $\widehat{S}_\alpha^U$ below.

Define the order statistics of the observations $\{\widehat{U}_1, \ldots, \widehat{U}_n\}$: $U_{1:n} \leq, \ldots, \leq U_{n:n}$. I use the choice of k, the number of upper order statistics included in the estimators $\hat{x}_\alpha^U$ and $\widehat{S}_\alpha^U$, as stated in Hoga (2019). The method for choosing this k is given in Appendix A.

Hoga (2019) gives the following estimator for the (1-α)-quantile ($\hat{x}_\alpha^U$) and the expected shortfall ($\hat{S}_\alpha^U$) of U_i using top order statistics:

$$\hat{x}_\alpha^U := U_{n-k:n} \left(\frac{n\alpha}{k} \right)^{-\hat{\gamma}} \tag{8}$$

$$\widehat{S}_{\alpha}^{U} := \frac{\widehat{x}_{\alpha}^{U}}{1-\widehat{\gamma}}, \tag{9}$$

where $U_{n-k:n}$ is the $(n-k)$th order statistic and $\hat{\gamma}$ the extreme value index. There are two potential estimators for γ. The Hill estimator of Hill (1975):

$$\widehat{\gamma}_H := \frac{1}{k}\sum_{i=0}^{k} \log\left(\frac{U_{n-i:n}}{U_{n-k:n}}\right). \tag{10}$$

Alternatively, $\hat{\gamma}$ can be estimated with the MR estimator of Danielsson et al. (1996) with

$$\widehat{\gamma}_{\mathrm{MR}} := \frac{1}{2}\frac{\frac{1}{k}\sum_{i=0}^{k}\left\{\log\left(U_{n-i:n}\right)-\log\left(U_{n-k:n}\right)\right\}^2}{\widehat{\gamma}_H}. \tag{11}$$

$\gamma > 0$ is required due to some restrictions and $\gamma < 1$ is required for ES to be finite. All the above combined results in the following point estimators for the CVaR and the CES:

$$\widehat{x}_{\alpha,n} = \widehat{\mu}_{n+1} + \widehat{\sigma}_{n+1}\widehat{x}_{\alpha}^{U}, \tag{12}$$

$$\widehat{S}_{\alpha,n} = \widehat{\mu}_{n+1} + \widehat{\sigma}_{n+1}\widehat{S}_{\alpha}^{U}, \tag{13}$$

respectively.

I do not include the first few residuals in the estimation as they are possibly affected by initialization effects. Also, in some cases, the last few observations are excluded as well. We include the subsample $\widehat{U}_{m_n}, \ldots, \widehat{U}_{\lfloor nt \rfloor}$, where $0 < t \leq 1$ is the fraction of elements omitted.By using EVT some last observations are excluded by specifying t. We define $\widehat{x}_{\alpha,n}(t)$ and $\widehat{S}_{\alpha,n}(t)$ as the estimators where $\hat{x}_{\alpha}^{U}$ and $\hat{S}_{\alpha}^{U}$ are calculated using observations until $\widehat{U}_{\lfloor nt \rfloor}$. Where k is replaced by $\lfloor kt \rfloor$.

Theorem 1 in Hoga (2019) suggests that under mild conditions, which can be found in their paper, the following (1-τ)-confidence interval can be calculated:

$$I_{\mathrm{na}}^{1-\tau} := \left[\widehat{z}_{\alpha,n}(1)\exp\left\{-\Phi\left(1-\frac{\tau}{2}\right)\widehat{\sigma}_{\hat{\gamma},\gamma}\frac{\log(k/(n\alpha))}{\sqrt{k}}\right\}, \widehat{z}_{\alpha,n}(1)\exp\left\{\Phi\left(1-\frac{\tau}{2}\right)\widehat{\sigma}_{\hat{\gamma},\gamma}\frac{\log(k/(n\alpha))}{\sqrt{k}}\right\}\right] \tag{14}$$

where $z \in \{x, S\}$, and na stands for the method of normal approximation which is used. $\Phi(\cdot)$ indicates the distribution function of a normal distribution. $\widehat{z}_{\alpha,n}(1)$ is the estimator for CVaR or CES where $t = 1$, meaning all last observations are included in the estimation. The interval can also be computed using the idea of self normalization which gives the following equation:

$$I_{\mathrm{sn}}^{1-\tau} := \left[\widehat{z}_{\alpha,n}(1)\exp\left\{\sqrt{V_{t_0,1-\tau}\int_{t_0}^{1} t^2\log^2\left(\frac{\widehat{z}_{\alpha,n}(t)}{\widehat{z}_{\alpha,n}(1)}\right)\mathrm{d}t}\right\}, \widehat{z}_{\alpha,n}(1)\exp\left\{-\sqrt{V_{t_0,1-\tau}\int_{t_0}^{1} t^2\log^2\left(\frac{\widehat{z}_{\alpha,n}(t)}{\widehat{z}_{\alpha,n}(1)}\right)\mathrm{d}t}\right]\tag{15}$$

Here, $\widehat{z}_{\alpha,n}(t)$ is the estimator for CVaR or CES as mentioned above, where t determines the fraction of observations left out of the estimation subsample $\widehat{U}_{m_n}, \ldots, \widehat{U}_{\lfloor nt \rfloor}$. t_0 is the lowest t we use. $V_{t_0,1-\tau}$ is the (1-τ)-quantile of V_{t_0} which is defined as follows:

$$V_{t_0} = \frac{W^2(1)}{\int_{t_0}^{1}[W(t) - tW(1)]^2\ \mathrm{d}t},\tag{16}$$

where $W(\cdot)$ is a standard Brownian motion.

2.3 Simulation study

I conduct a simulation study where I examine the coverage of the CVaR and CES intervals for a sample series of $n = 1000$ observations. I use $t_0 = 0.2$ so the minimal sample size is 200. To prevent invalidity of the CES estimate I follow Hoga (2019) and use $\widehat{S}_\alpha(t) = \widehat{x}_\alpha^U(t)/(1 - \min\{\widehat{\gamma}(t), 0.9\})$. Furthermore, I use the same settings as Hoga (2019): 10,000 replications, $\alpha = 2, 5\%, 1\%, 0.5\%$ and $m_n = 10$. For the choice of k, formula (27) is used, where $k_{min} = 50$ and $k_{max} = 200$. The following three models are simulated:

$$X_i = \varepsilon_i, \quad \text{where} \quad \varepsilon_i = \sigma_i U_i, \quad U_i \sim st_3(5), \quad \sigma_i^2 = 0.95\cdot\frac{20^2}{252} + 0.15\cdot\varepsilon_{i-1}^2 + 0.8\cdot\sigma_{i-1}^2\tag{17}$$

$$X_i = \varepsilon_i, \quad \text{where} \quad \varepsilon_i = \sigma_i U_i, \quad U_i \sim st_{4.2}(0), \quad \sigma_i^2 = 3.2\cdot 10^{-6} + 0.0349\cdot\varepsilon_{i-1}^2 + 0.9373\cdot\sigma_{i-1}^2,\tag{18}$$

$$X_i = 0.2714X_{i-1} + \varepsilon_i, \quad \text{where} \quad \varepsilon_i = \sigma_i U_i, \quad U_i \sim st_{5.3}(0.8531), \quad \sigma_i^2 = 3.4\cdot 10^{-6} + 0.1407\cdot\varepsilon_{i-1}^2 + 0.7914\cdot\sigma_{i-1}^2.\tag{19}$$

Here, $st_\nu(\xi)$ means U_i is distributed with a skewed Student's t distribution with ν degrees of freedom and ξ the skewness parameter. If $\xi = 0$, the skewed Student's t distribution simplifies to a Student's t distribution. As stated in section 2.1, unit variance of the innovation terms is assumed. Therefore, I standardise the sampled U_i by subtracting the mean and dividing by the standard deviation.

2.4 Empirical application

I investigate what the best methods are to estimate the CVaR and CES for cryptocurrencies. Therefore, I apply the method developed to loss returns of three different cryptocurrencies: Bitcoin (BTC), Ethereum (ETH) and Ripple (XRP). Also, I apply the methodology to an index of cryptocurrencies, the Cryptocurrency Index (CRIX). I compare the results to 3 global indices in the stock market: the NASDAQ from North America, the Nikkei 225 from Asia and the CAC 40 from Europe.

3 Data

For the three global indices NASDAQ, Nikkei 225, and CAC 40, I downloaded data from finance.yahoo.com for the period 1/1/1997 to 31/12/2016, following Hoga (2019). These indices are not traded 24/7 and on some days (holidays etc) the markets are closed and no stocks or indices are traded. This means there are missing observations in the data. For the NASDAQ composite, I downloaded 5034 observations, for the Nikkei 25 5052 observations, and for the CAC 40 5159 observations. As these indices belong to different regions in the world they are open and closed on different days.

For the three cryptocurrencies, I got their closing prices from coindesk.com. As these cryptocurrencies are a much newer asset class than the stock indices it is not possible to download the data for the same timeframe. I decided to download the cryptocurrency data for the entire period of their existence. This means for Bitcoin I used the period 1-10-2013 to 7-5-2021 (2761 observations). For Ethereum I used the period 9-8-2015 to 7-5-2021 (2084 observations). For Ripple, I used the period 3-7-2014 to 7-5-2021 (1058 observations). For the CRIX I downloaded the closing data from data.thecrix.de for the time period 3-7-2014 to 6-5-2021 (2472 observations).

Figure 1 shows the closing prices of the three indices. The closing prices are adjusted for dividends and splits. We see that the indices move in the same direction even though they originate from different markets in different areas of the world. The figure shows that the N225 reacts much more to events in the market than the other two indices. It is more volatile.

Figure 2 shows the closing prices of the three cryptocurrencies. Bitcoin was created much earlier than the other two cryptocurrencies, so it already had a higher closing price when later the other two were created. Therefore the Bitcoin is more known and this could be a reason why its closing

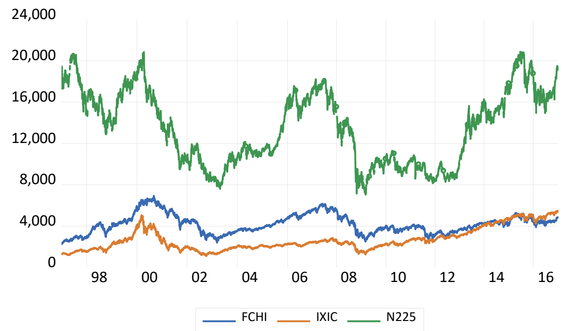

Figure 1: Closing prices of CAC40 (FCHI), NASDAQ composite (IXIC) and Nikkei 225 (N225)

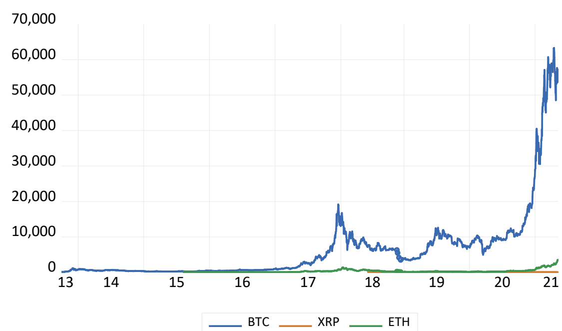

Figure 2: Closing prices of Bitcoin (BTC), Ethereum (ETH) and Ripple (XRP)

price is much higher than the other two. The graphs of the prices of the cryptocurrencies separately can be found in the appendix. Bitcoin seems to be the most volatile currency.

Table 1 shows the summary statistics of the log returns of the three global stock indices, the three cryptocurrencies and the cryptocurrency index respectively. We observe from the CRIX column very extreme values for the minimum and maximum, the skewness, kurtosis and the Jarque-Bera statistic. When we have a look at the graph of the closing prices of this index (given in the appendix), we see one very big outlier at 25/03/2021. This outlier is probably the cause of the remarkable values. Indeed, if we remove this observation from the data we get the statistics as presented in the last column. These are much more logical as these are comparable to the properties of the three cryptocurrencies.

We can observe from the first three columns that the three indices have comparable properties. Which we would expect when inspecting the graphs of the closing prices mentioned earlier. The three cryptocurrencies are also comparable in their characteristics. But if we compare the cryptocurrencies to the global indices we observe that the cryptocurrencies have larger standard deviations, larger skewness and larger kurtosis. These assets therefore are more volatile and more likely to produce large negative or large positive returns. All of the assets have a very high Jarque-Bera statistic with p-values equal to zero. This means that the returns do not follow a normal distribution. Thus it would not be suitable to use a normal distribution when estimating the returns. It would be wiser to use a heavy-tailed distribution like (skewed) Student's t or a Laplace distribution.

Table 1: Summary statistics of global stock indices, cryptocurrencies and the cryptocurrency index

	IXIC	**N225**	**FCHI**	**BTC**	**ETH**	**XRP**	**CRIX**	**CRIX Adjusted**
Mean	0.000	0.000	0.000	0.002	0.004	0.001	0.002	0.002
Maximum	0.133	0.132	0.106	0.306	0.433	0.370	2.748	0.214
Minimum	-0.102	-0.121	-0.095	-0.316	-0.424	-0.450	-2.811	-0.447
St. dev	0.016	0.015	0.015	0.043	0.065	0.056	0.089	0.040
Skewness	-0.056	-0.349	-0.069	-0.440	0.233	0.510	-0.989	-0.788
Kurtosis	8.170	8.539	7.320	10.322	9.731	14.855	783.884	14.133
Jarque-Bera	5608.441	6217.795	3929.194	6255.007	3951.282	6235.181	62782359	13010.570
p-value	0.000	0.000	0.000	0.000	0.000	0.000	0.000	0.000

Note: The table shows summary statistics of three major global stock indices (the NASDAQ composite, the Nikkei 225, and the CAC40), three cryptocurrencies (Bitcoin, Ethereum, Ripple) and a cryptocurrency index (CRIX) respectively. The last column represents the statistics of the CRIX where the observation of 25/03/2021 is removed.

I will work with loss-returns which I calculate manually from the closing prices according to the following formula:

$$X_i = -log(P_t/P_{t-1}), \tag{20}$$

where P_t is the closing price of the asset at time t.

4 Simulation results

We first estimate quantiles of V_{t_0}. Table 2 shows the result of the simulation.

Table 2: Quantiles $V_{t_0,\tau}$ of V_{t_0}

τ	t_0	0.50	0.60	0.70	0.80	0.90	0.95	0.975	0.99	0.995
V_{t_0}	0.3	4.557	7.572	12.641	21.127	41.094	65.851	99.408	149.155	189.821
	0.2	3.940	6.479	10.760	17.990	34.316	56.752	84.935	130.803	157.779
	0.1	3.522	5.924	9.672	16.089	30.424	48.207	72.089	105.301	138.345

For the simulations I used an adapted version of the code belonging to Hoga (2019). A point of criticism on Hoga (2019) can be made. They use information on the data generating process in there simulation. However, this is a little dishonest. Therefore in my simulations, I considered the simulated data as 'given' and did not use information on the process in the estimation. I estimated a GARCH(1,1) model for all three simulations. The results of these simulation can be found in table 3. A table with the simulation results following the methodology of Hoga (2019) can be found in Appendix C.

From table 3 we observe that the use of the MR estimator, instead of the Hill estimator, considerably lowers the RMSE for most of the values for α and the three models. Only for model 17 for α equal to 1% and 0.5% the RMSE is not improved when using the MR estimator.

Nominal coverage for all intervals is 95%. For all models, the MR estimator substantially improves the coverage of the intervals created by normal approximation (na in the table). For the intervals constructed by using self normalization (sn in the table), this is not the case. Here, the coverage of the intervals is worse for the MR estimator compared to the Hill estimator for two of the three models (model 18 and model 19). But the improved coverage for the MR estimator for the na intervals comes at the cost of much-enlarged intervals. Most interval lengths are doubled in size for the MR estimator when compared to the Hill estimator. Therefore, the intervals give a less precise estimate for the CVaR or CES values.

When we compare the method of normal approximation to that of self normalization, most of the time the coverage improves when using the self normalization approach. Only for models 18 and 19, the self normalization approach combined with the MR estimator gives worse coverage. So we can conclude that using self normalization, in general, improves the coverage of the constructed intervals.

Lastly, we study the influence of the level of α. For model 17, larger values of α give smaller bias and RMSE. For model 18, for the Hill estimator, larger values of α give smaller and RMSE. But for the MR estimator, for larger α, the CVaR estimates give larger bias, but the CES estimates give smaller bias. For the RMSE the results are more mixed, where values of RMSE are largest for α equal to 1%. In general, larger values for α give smaller bias and RMSE.

According to Theorem 1 of Hoga (2019) the following approximations hold:

$$\frac{1}{\widehat{\sigma}_{\hat{\gamma},\gamma}} \frac{\sqrt{k}}{\log(k/(n\alpha))} \log\left(\frac{\widehat{z}_{\alpha,n}(1)}{z_{\alpha,n}}\right) \underset{(n\to\infty)}{\xrightarrow{D}} \mathcal{N}(0,1), \text{ and} \tag{21}$$

$$\frac{\log^2\left(\frac{\widehat{\hat{z}_{a,n}(1)}}{z_{\mathrm{a},n}}\right)}{\int_{t_0}^1 t^2 \log^2\left(\frac{\widehat{Z}_{\sigma,n}(t)}{z_{a,n}(1)}\right) \mathrm{d}t} \; (n \overset{\mathcal{D}}{\to} \infty) \; \frac{W^2(1)}{\int_{t_0}^1 [W(t) - tW(1)]^2 \; \mathrm{d}t} =: V_{t_0}. \tag{22}$$

Table 3: Simulation results for the three simulation models 17, 18 and 19.

							Coverage		Int. length	
Model	Estimator	$k*$	z	α	Bias	RMSE	$I_{na}^{0.95}$	$I_{sn}^{0.95}$	$I_{na}^{0.95}$	$I_{sn}^{0.95}$
17	Hill	67	CVaR	2.5%	-0.18	1.30	14.6	53.9	0.13	0.77
				1%	-0.34	1.17	12.1	63.4	0.15	1.30
				0.5%	-0.53	1.86	11.9	66.3	0.16	2.63
			CES	2.5%	-0.38	2.42	19.9	65.4	0.35	5.88
				1%	-0.53	1.66	22.4	73.8	0.46	3.10
				0.5%	-0.69	2.64	21.7	74.2	0.52	17.60
	MR	93	CVaR	2.5%	-0.07	1.22	43.1	60.2	0.54	0.91
				1%	-0.22	1.10	45.7	69.6	0.78	1.45
				0.5%	-0.40	1.82	45.1	69.6	1.08	5.31
			CES	2.5%	-0.22	1.67	38.3	67.4	0.69	1.49
				1%	-0.40	1.69	39.6	74.7	1.09	4.05
				0.5%	-0.57	3.26	38.3	74.1	1.83	331.69
18	Hill	58	CVaR	2.5%	-0.78	5.94	25.6	73.0	3.37	6.96
				1%	-2.08	13.94	24.4	79.6	4.61	13.96
				0.5%	-3.40	11.16	26.9	83.1	5.71	23.64
			CES	2.5%	-3.40	10.42	70.1	83.3	11.33	19.72
				1%	-7.73	26.45	64.3	86.5	18.52	39.03
				0.5%	-11.57	22.37	57.7	85.1	25.72	62.91
	MR	62	CVaR	2.5%	0.33	5.62	89.6	68.3	13.69	7.34
				1%	0.21	12.72	88.9	71.7	22.09	13.34
				0.5%	0.00	9.41	90.5	74.4	30.24	20.99
			CES	2.5%	-0.45	8.68	87.7	76.0	20.37	16.09
				1%	-2.08	22.65	87.3	81.3	33.21	31.88
				0.5%	-4.27	17.36	88.2	83.6	45.73	49.75
19	Hill	58	CVaR	2.5%	-1.05	4.13	18.4	42.8	1.31	3.01
				1%	-1.74	6.92	20.9	58.7	1.69	5.61
				0.5%	-0.80	2.93	32.4	89.5	1.72	8.06
			CES	2.5%	-2.39	6.05	38.3	62.0	3.79	7.37
				1%	-4.12	10.42	41.4	75.7	5.66	13.69
				0.5%	-3.16	5.79	48.8	91.0	6.32	17.87
	MR	67	CVaR	2.5%	-0.46	3.80	62.6	44.7	5.05	3.27
				1%	-0.64	6.22	69.5	54.1	7.36	5.39
				0.5%	0.75	2.18	84.3	70.9	6.22	4.70
			CES	2.5%	-1.09	5.07	65.0	59.5	6.82	6.28
				1%	-2.01	8.74	70.1	68.6	9.95	11.12
				0.5%	0.00	3.06	85.8	85.2	8.30	9.33

The table shows in the columns the average of $k*$, bias RMSE, coverage probabilities in %, and average interval lengths for the Hill and MR estimator respectively. For simulation models 18 and 19, the results are multiplied by 10^3.

These approximations determine the quality of the na and sn intervals respectively. To asses this quality, I plot the left and right hand side of these approximations in a probability-probability plot. The more the plot follows the diagonal line, the more accurate the approximation. Figure 3 shows the pp-plot for model 18 for the CES estimates and $\alpha = 0.01$. The results for model 17 and 19 can be found in Appendix B. Results for other values for α or for CVaR estimates can be requested from the author of this paper.

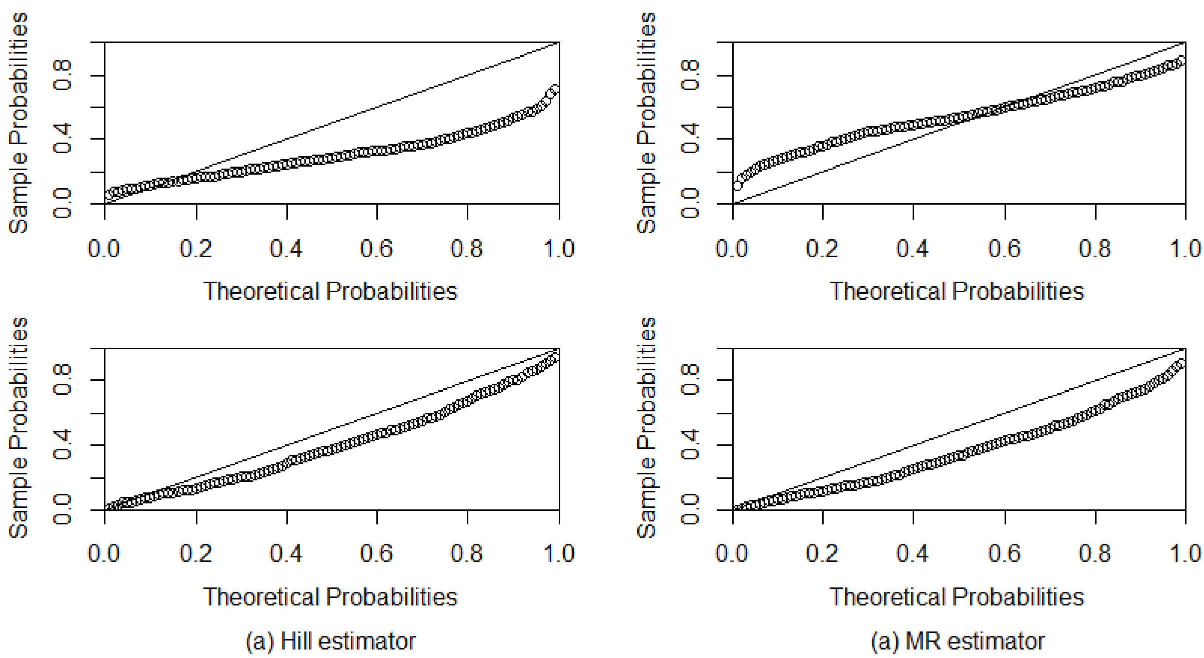

Figure 3: Probability-probability plots for left and right hand side of 21 and 22 for model 18.

In Figure 3 , the top row resembles equation 21 for normal approximation and the bottom two graphs represent equation 22 for self normalisation. We observe that the self normalization is a better fit to the empirical distribution for both the Hill and the MR estimator. Consistent with the findings in Table 3 we see that, for the normal approximation, the MR estimator follows the empirical distribution better than the Hill estimator. For self normalization, this seems to be the other way around.

We furthermore investigated what the influence of k is on the simulation results. Plots for the coverage, interval length, bias ,and RMSE for all possible $k \in \{50, ..., 200\}$ are depicted in figure 4 for model 17. For model 18 the results can be found in Appendix B and show a similar result. For model 19 the results are very similar and therefore omitted, but can be requested from the author.

Figure 4 shows that the choice of k heavily influences the coverage, interval lengths, bias, and

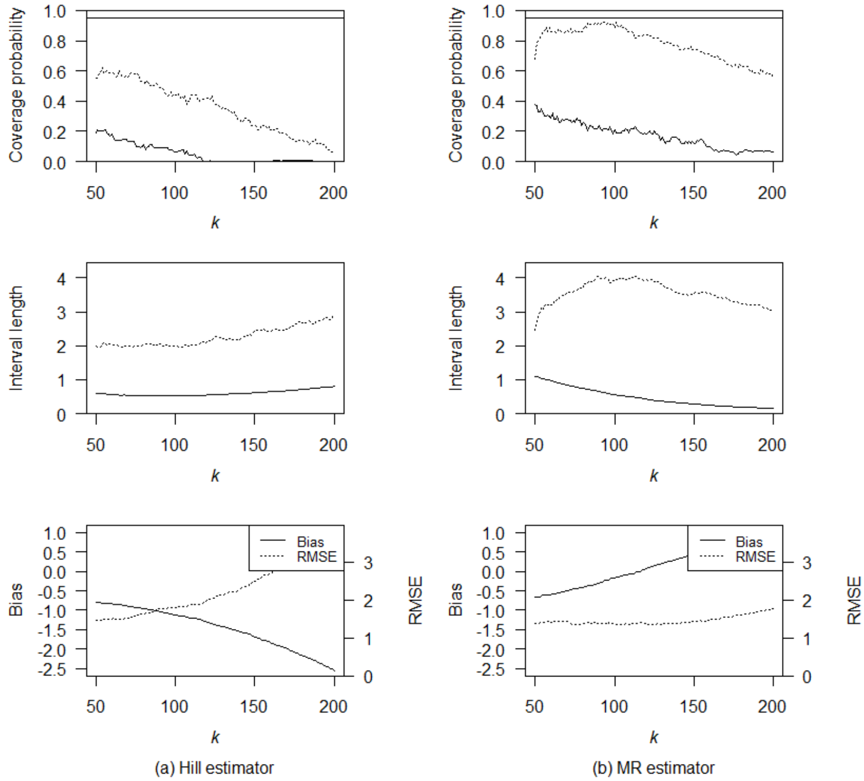

Figure 4: Simulation results for model 17 as a function of k
(a) Coverage probabilities, and interval lengths as functions of k, for 1% CES estimates for model 17. The solid line depicts intervals based on normal approximation and the dotted line represents intervals based on self normalisation. The horizontal line in the top plots depicts the nominal coverage of 95%. The bottom plots depict the bias (solid, left scale) and RMSE (dotted, right scale) for the Hill estimator. (b) Everything the same but for the MR estimator.

RMSE for the Hill estimator. For the MR estimator the choice of k has smaller influence on the results. Consistent with the results in table 3 we observe that the value of k for which coverage is highest, is higher for the MR estimator than for the Hill estimator.

From the simulation results, we conclude that, overall, the MR estimator improves coverage for both the na and sn intervals. Also using self normalization instead of normal approximation considerably improves coverage. However, the coverage for the Hill estimator seems to give a more reliable result. To summarise, using the Hill estimator in combination with the self normalization approach proves to be the best method.

5 Application

5.1 Stock indices

Table 4: Backtesting CVaR and CES forecasts of global stock indices

Index	Method	UC	CC	Quantile score	AL log score
NASDAQ	G-k-H	0.1687	0.0967*	0.9527	-8489.1
	AG-$k*$-H	0.4798	0.1136	**0.9411**	**-8598.2**†
	AG-$k*$-MR	0.1927	0.0006***	0.9462	-8501.6
Nikkei 225	G-k-H	0.4989	0.0902*	1.1030	-7135.2
	AG-$k*$-H	0.8294	0.0000***	**1.0993**	**-7168.6**
	AG-$k*$-MR	0.2432	0.0000***	1.1060	-7110.3
CAC 40	G-k-H	0.2429	0.9997	1.0157	-8219.5
	AG-$k*$-H	0.9573	0.9925	**1.0090**	**-8264.7**
	AG-$k*$-MR	0.2888	0.0097***	1.0112	-8178.2

*The table shows in the columns p-values of the backtests of Berkowitz et al. (2011) (CC) (significance at 10%,5%, and 1% marked with *, **, and ***), Quantile scores and AL log scores respectively.*

For an application of the constructed procedure, we apply the methods to three major global stock indices. We introduce 3 different models to investigate their fit to the stock index data. The first model comprises a GARCH(1,1) model with a fixed value for k and the use of the Hill estimator. k is equal to $\lfloor 1.5(log(n))^2 \rfloor$. The second model uses an AR(1)-GARCH(1,1) model with the data-driven choice of k proposed by Hoga (2019) using the Hill estimator. The third model uses an AR(1)-GARCH(1,1) model with the data-driven choice k too but uses the MR estimator in calculating the optimal k and the estimators.

Table 4 shows the results of the backtesting procedures. We use rolling forecasts for a window of n equals 1000 for the estimation sample. For days $j \in n, ..., N-1$ we forecast the CVaR and CES estimates $x_i^{(m)}$ and $S_i^{(m)}$ respectively. Where N denotes the total number of observations in the entire time series.

We then test the quality of these forecasts by checking the amount of data entries that exceed the forecasted CVaR value (called violations from now). These violations should be independently Bernoulli distributed with success probability α. We use the test of Kupiec (1995) (UC in the table) which tests the unconditional coverage; if the expected amount of violations indeed is approximately equal to α. Second, we test for independence of the violations where we use the test of Berkowitz et al. (2011) (CC in the table). To compare the absolute performance between models, we introduce two statistics. We use two scoring functions which quantify the loss associated with a forecast.

Therefore lower values are preferred. The scoring functions I use are the *quantile score* and the *asymmetric Laplace (AL) log score*. The quantile score is calculated as:

$$S_{\text{VaR}}\left(x_i, X_i\right) = \left(X_i - x_i\right)\left(\alpha - I_{\{X_i \leq x_i)}\right), \tag{23}$$

The AL log score is calculated as:

$$S_{\text{ES}}\left(x_i, S_i, X_i\right) = -\log\left(\frac{\alpha - 1}{S_i}\right) - \frac{\left(X_i - x_i\right)\left(\alpha - I_{[X_i \leq x_i\}}\right)}{\alpha S_i}. \tag{24}$$

Here, x_i denotes the forecasted CVaR, S_i denotes the estimated CES and X_i denotes data, where I use the loss returns.

We report in the table the realised scores which are calculated as:

$$\bar{S}_{\text{VaR}}^{(m)} = \frac{1}{N-n}\sum_{i=n+1}^{N} S_{\text{VaR}}\left(x_i^{(m)}, X_i\right) \quad \text{and} \tag{25}$$

$$\bar{S}_{\text{ES}}^{(m)} = \frac{1}{N-n}\sum_{i=n+1}^{N} S_{\text{ES}}\left(x_i^{(m)}, S_i^{(m)}, X_i\right) \tag{26}$$

Where we use the quantile score to evaluate the CVaR forecasts and the AL log score to evaluate the CES forecasts. I printed the lowest values in the table bold. From Table 4 we observe that the model AG-$k*$-MR is always rejected based on independence. The other two models seem more satisfactory. For two of the three stock indices, the AG-$k*$-H model is never rejected for all the significance levels.

From the table, we can deduce that for all three stock indices, the AG-$k*$-H model performs best in forecasting the CVaR and CES. Lastly, we perform the test of Diebold and Mariano (2002) to test the significance between the realized scores for the first model and the second model. I left the third model out of consideration as we already observed this model as not very suitable. In the table, I denoted a significant difference (5% level) with a dagger. We conclude from the results that the AG-$k*$-H model performs the best for global stock index data. The use of the MR estimator does not enhance the performance of the models when compared to the Hill estimator.

Table 5: Backtesting CVaR and CES forecasts of cryptocurrencies

Index	Method	UC	CC	Quantile score	AL log score
BTC	G-k-H	0.0633*	0.0008***	2.0385	-1000.3
	AG-$k*$-H	0.0633*	0.0008***	1.9445†	-1153.6†
	AG-$k*$-MR	0.3055	0.0029***	**1.8312**	**-1166.3**
ETH	G-k-H	0.1765	1	1.7575	-289.8
	AG-$k*$-H	0.8695	0.0000***	**1.7064**	**-394.8**†
	AG-$k*$-MR	0.0271**	0***	1.7824	-311.8
XRP	G-k-H	0.8010	1.000	**0.3886**	-70.6
	AG-$k*$-H	0.5272	0***	0.3904	-78.2
	AG-$k*$-MR	0.5272	0***	0.4295	**-79.6**
CRIX	G-k-H	0.6384	0.9998	4.7248	**1643.7**
	AG-$k*$-H	0.9020	0.9993	**4.6329**	1658.2
	AG-$k*$-MR	0.3590	0.9894	4.6486	2143.5

*The table shows in the columns p-values of the backtests of Berkowitz et al. (2011) (CC) (significance at 10%,5%, and 1% marked with *, **, and ***), Quantile scores and AL log scores respectively.*

5.2 Cryptocurrencies

In addition to stock indices, I apply the methods to three different cryptocurrencies and to one cryptocurrency index. For these series, I used an estimation window of $n = 800$ because for the cryptocurrencies, there is very limited data available due to the short existence of the currencies.

Table 5 shows results for the backtests of the CVaR and CES forecasts. From the table, we observe that based on the unconditional coverage test of Kupiec (1995) and the independence test of Berkowitz et al. (2011) there is not a clear method that works best. For Bitcoin, all of the models are rejected based on the independence of the violations. For Ethereum and Ripple, the model using the fixed value for k and the GARCH(1,1) model is never rejected. When we examine the quantile scores, we observe that for every cryptocurrency another model gives the lowest value for the quantile score. This also accounts for a part for the AL log score. Therefore we can not deduce from this analysis which model or method gives consistently better predictions. When we examine the cryptocurrency index (which gives a more general image of the cryptocurrencies in general), it rejects no model based on the correct unconditional coverage test or the independence test. The model using the data dependent varying k and the Hill estimator gives the lowest value for the quantile score. The benchmark GARCH(1,1) model using fixed k gives the lowest value for the AL log score.

We try to find a explanation why for Bitcoin, none of the models seem to work. When we look at the first (benchmark) model, G-k-H , we plot the data (loss-returns) with the forecasted VaR values in Figure 5 to be able to examine the violations. A violation happens when the loss return is higher than the forecasted VaR value for that period. For Bitcoin we observe only four violations: at the times 11/6/2018, 14/11/2018, 20/11/2018 and 11/3/2020.

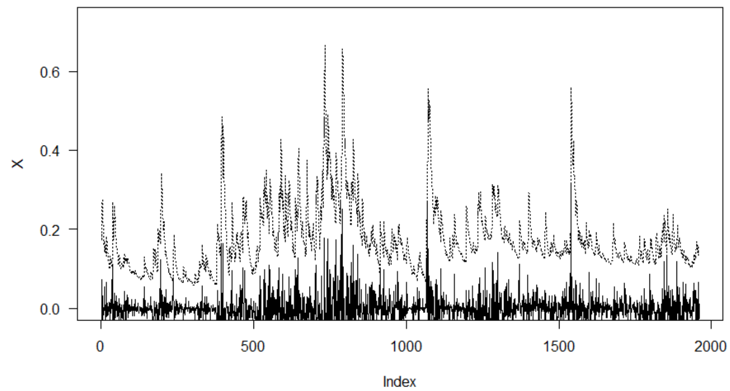

Figure 5: Loss returns for Bitcoin (solid) and the forecasted VaR values (dotted) for the forecast period 11/12/2015 - 7/5/2021.

We tried to connect these dates to news around Bitcoin or cryptocurrency. On 10/6/2018, the South Korean cryptocurrency exchange Coinrail was hacked. Therefore, during 10/6/2018, the price of Bitcoin declined from 7531.98 USD to 6786.02 USD (9% decrease). However, on 11/6/2018 the price went up again to 6906.92 USD. None of the models accurately predicted this increase. 14/11/2018 was the start of a large, fast decrease of the price of Bitcoin. It was the end of what became known as the Bitcoin crash which started in the beginning of 2018 and ultimately became larger than the burst of the Dot-Com bubble. On 15/11/2018, the Market capitalisation of Bitcoin fell below $100 billion for the first time since October 2017. Also, that day a Bitcoin hard Fork happened with Bitcoin Cash, which is a different cryptocurrency created by another hard fork of Bitcoin which happened in August 2017. The end of the sharp decrease of the price of Bitcoin seemed to be 21/11/2018. There does not seem to be an obvious reason why the models where not able to predict this occurrence correctly. However, all models are rejected based on the argument of independence. We could argue that this is caused by the fact that there are only very few violations, and two of those violations (14/11/2018 and 21/11/2018) are rather close to each other. Leading to the CC test rejecting the model. The last violation on 11/3/2020, happened alongside a large sell off which happened in other markets as well due to the Corona virus breakout. For example, in the stock market, the S%P 500 decreased with 5%, the oil price fell by 4%, and even the Gold price was down 1%, which is regarded by many investors as a 'safe haven'.

For Ethereum and Ripple, the benchmark GARCH(1,1) model with fixed k performs well. To investigate further why the other models do not work, we examined the values for $k*$ for the Hill and MR estimators. The value of fixed k for n equals 800 is 67. The mean values for $k*$ for Ethereum are 54 and 66 for the Hill and MR estimator respectively. The value for the MR estimator is very close to the value for the fixed k so this does not explain why the model does not perform well. To investigate further, we plot the values for $k*$ for all forecasted values. Figure 6 shows that the value for $k*$ varies a lot and is most of the time far away from 67. For Ripple the mean values for $k*$ are 61 and 50 for the Hill and MR estimator respectively. The value for the MR estimator is too small. The $k*$ searches for the optimal number of upper order statistics to resemble a Pareto distribution. However, when there are very large outliers present in the data, the upper order statistics do not resemble a Pareto distribution, which drives the $k*$ down by much. As there are indeed more outliers in cryptocurrency data than for example in stock index data, as shown in section 3, this causes the very low values for $k*$ which is illustrated by Figure 6.

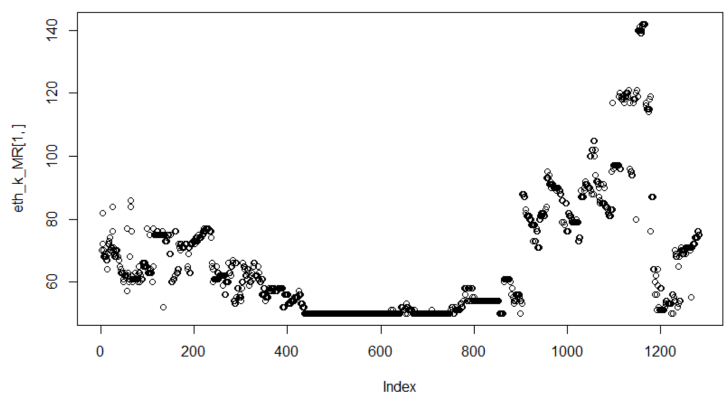

Figure 6: Values for $k*$ for the MR estimator for the forecast sample.

For the Cryptocurrency index these values are 54 and 68 which are much closer to the fixed k. This could be a reason why for Ethereum and Ripple the models with $k*$ do not work and for the Cryptocurrency index they do.

To investigate further, I applied four more models; AR(1)-GARCH(1,1) with fixed k and the Hill estimator (AG-k-H), AR(1)-GARCH(1,1) with fixed k and MR estimator (AG-k-MR), GARCH(1,1) with $k*$ and Hill estimator (G-$k*$-H) and GARCH(1,1) with $k*$ and MR estimator (G-$k*$-MR). The results are presented in Table 6

Table 6: Backtesting results for additional models

Index	Method	UC	CC	Quantile score	AL log score
ETH	AG-k-H	0.3391	0.9999	-1.7720	-238.0
	AG-k-MR	0.0271**	0***	-1.7687	-344.7
	G-$k*$-H	0.8695	0.000***	-1.6960	**-406.7**
	G-$k*$-MR	0.0271**	0***	**-1.7910**	-308.9
XRP	AG-k-H	0.8010	1.000	**0.3886**	-69.4
	AG-k-MR	0.5271	0***	0.4184	**-82.1**
	G-$k*$-H	0.5271	0***	0.3912	-78.2
	G-$k*$-MR	0.5271	0***	0.4304	-79.2

*The table shows in the columns p-values of the backtests of Berkowitz et al. (2011) (CC) (significance at 10%,5%, and 1% marked with *, **, and ***), Quantile scores and AL log scores respectively.*

From Table 6 we conclude that models with $k*$ never work for Ethereum and Ripple. Furthermore, from the table we deduce that the Hill estimator does give well performing models, where the MR estimator does not.

From the cryptocurrency application we conclude that the use of the MR estimator does not improve forecasts of CVaR and CES. This is in line with the findings from the application to stock indices. Also the use of an optimal $k*$ which is calculated from the data is not a suitable approach for forecasting the CVaR and CES of cryptocurrency data. A disadvantage is that for cryptocurrencies a lot less data is available than for stock indices as most cryptocurrencies are very new. Therefore there are also very few data points available to use for forecasting and evaluation.

6 Conclusion

In this paper, we examined the influence of the moments Ratio (MR) estimator versus the Hill estimator in the forecasting of the CVaR and CES measures. From the simulation results, we found that the MR estimator does improve coverage of the estimated intervals for the CVaR and CES forecasts. However, it comes at the cost of larger intervals. Furthermore, the use of self normalization instead of normal approximation in constructing the intervals also improves the coverage of the intervals, but also enlarging the intervals. Therefore these intervals give a less precise view of the CVaR and CES values.

From the application to stock indices we found that the use of the Hill estimator leads to better performing models for forecasting the CVaR values for the returns of stock indices. This contradicts the findings of the simulation study, where we found that the MR estimator performs better than the Hill estimator. For the application to cryptocurrencies, we found similar results, as the use of the Hill estimator gave better results than the use of the MR estimator, as they gave lower scores and passed the backtests. Furthermore, we found that the use of the data-dependent method of choosing the upper-order statistics is not a good method for cryptocurrencies, as these assets prove to be incompatible with this choice. The larger amount of outliers present in the cryptocurrency data compared to the stock index data could be an explanation for this.

The results are of limited reliability as for the cryptocurrencies a lot less data is available compared to other asset classes like stocks or commodities. For future research, it would be interesting to look at other values or methods for choosing the number of upper-order statistics. There could also be research into how to keep the improved coverage of the MR estimator but also decreasing the interval length and with that, give more precise estimations for the CVaR and CES measures which is very relevant to investors and institutions who want to minimize their risk while still trying to get high returns.

References

J. Berkowitz, P. Christoffersen, and D. Pelletier. Evaluating value-at-risk models with desk-level data. *Management Science*, 57(12):2213–2227, 2011.

D. L. K. Chuen, L. Guo, and Y. Wang. Cryptocurrency: A new investment opportunity? *Journal of Alternative Investments*, 20(3):16–40, 2017.

J. Danielsson, D. W. Jansen, and C. G. De vries. The method of moments ratio estimator for the tail shape parameter. *Communications in Statistics-Theory and Methods*, 25(4):711–720, 1996.

F. X. Diebold and R. S. Mariano. Comparing predictive accuracy. *Journal of Business & economic statistics*, 20(1):134–144, 2002.

W. Feng, Y. Wang, and Z. Zhang. Can cryptocurrencies be a safe haven: a tail risk perspective analysis. *Applied Economics*, 50(44):4745–4762, 2018.

B. M. Hill. A simple general approach to inference about the tail of a distribution. *Annals of Statistics*, 3(5):1163–1174, 1975.

Y. Hoga. Confidence intervals for conditional tail risk measures in arma–garch models. *Journal of Business & Economic Statistics*, 37(4):613–624, 2019.

P. Kupiec. Techniques for verifying the accuracy of risk measurement models. *The J. of Derivatives*, 3(2), 1995.

W. Zhang, P. Wang, X. Li, and D. Shen. Some stylized facts of the cryptocurrency market. *Applied Economics*, 50(55):5950–5965, 2018.

Appendix A: supplementary formulas

Choice of k

$k_{\min}$ and $k_{\max}$ are the lower and upper bound for k respectively and $k_{\max} > k_{\min} \geqslant 1$.

$$k^* := \underset{k=k_{\min},\ldots,k_{\max}}{\arg\min} \left[\sup_{j=1,\ldots,k_{\max}} |U_{n-j,n} - q(j,k)| \right], \tag{27}$$

with $q(j,k) = U_{n-k,n} \left(\frac{j}{k}\right)^{-\hat{\gamma}}$ and $U_{n-j,n}$ is the observed quantile.

Appendix B: supplementary graphs

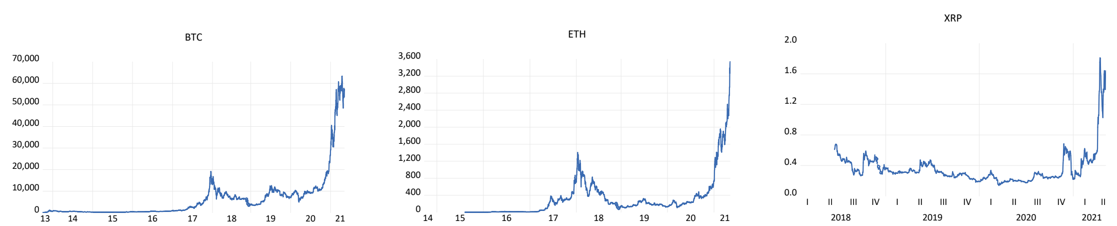

(a) Closing prices Bitcoin (b) Closing prices of Ethereum (c) Closing prices of Ripple

Figure 7: Closing prices of cryptocurrencies

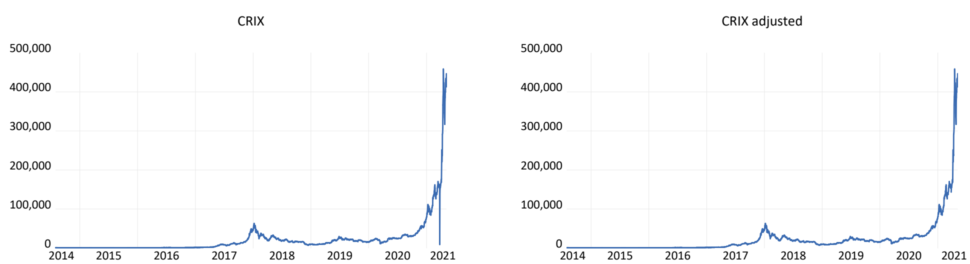

Figure 8: Closing prices of CRIX and the adjusted CRIX

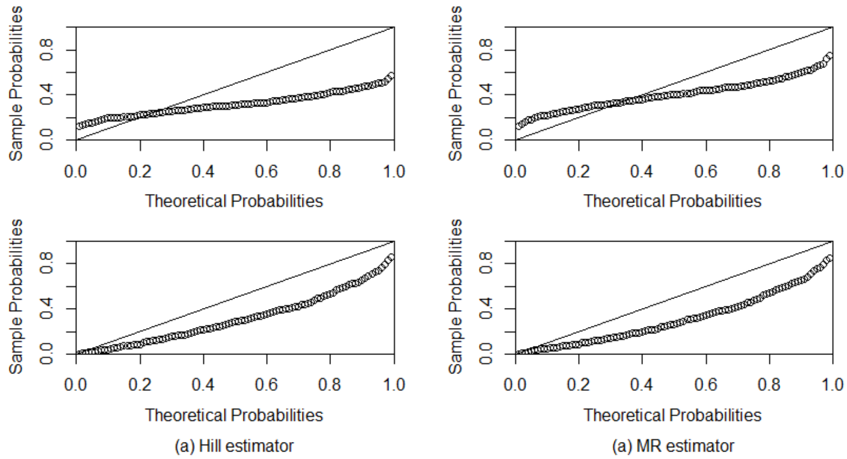

(a) Model 17

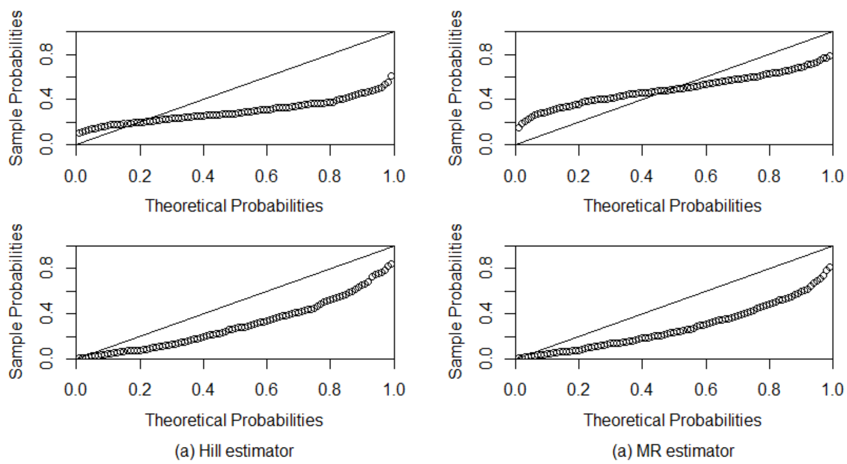

(b) Model 19

Figure 9: Probability-probability plots for left and right hand side of 21 and 22

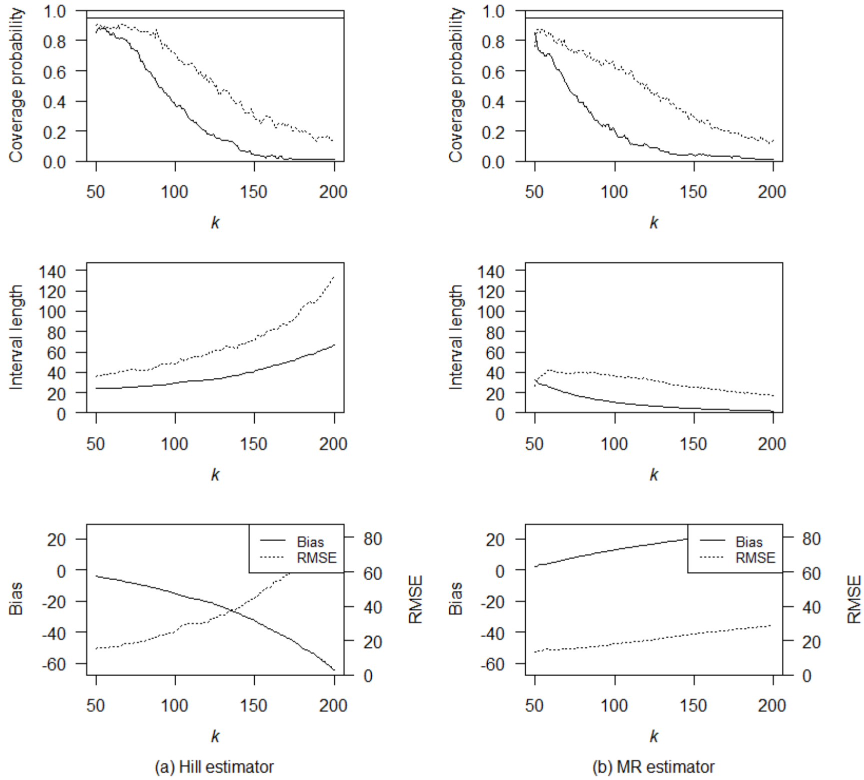

Figure 10: Simulation results for model 18 as a function of k
(a) Coverage probabilities, and interval lengths as functions of k, for 1% CES estimates for model 18. The solid line depicts intervals based on normal approximation and the dotted line represents intervals based on self normalisation. The horizontal line in the top plots depicts the nomial coverage of 95%. The bottom plots depict the bias (solid, left scale) and RMSE (dotted, right scale) for the Hill estimator. (b) Everything the same but for the MR estimator.

Appendix C: supplementary results

Table 7: Simulation results for the three simulation models 17, 18 and 19 following the methodology of Hoga (2019)

							Coverage		Int. length	
Model	Estimator	$k*$	z	α	Bias	RMSE	$I_{na}^{0.95}$	$I_{sn}^{0.95}$	$I_{na}^{0.95}$	$I_{sn}^{0.95}$
17	Hill	68	CVaR	2.5%	-0.00	0.51	20.4	72.1	0.09	0.48
				1%	-0.09	0.63	18.3	78.0	0.11	0.77
				0.5%	-0.19	1.13	13.9	84.7	0.12	1.17
			CES	2.5%	-0.04	0.59	33.5	81.4	0.22	0.91
				1%	-0.10	0.77	31.2	87.2	0.28	1.40
				0.5%	-0.15	1.36	28.7	89.8	0.35	1.97
	MR	77	CVaR	2.5%	0.08	0.52	56.8	73.7	0.36	0.63
				1%	-0.00	0.62	61.3	80.5	0.49	0.96
				0.5%	-0.10	1.04	57.9	83.9	0.60	1.37
			CES	2.5%	0.04	0.62	50.7	80.8	0.43	1.11
				1%	-0.01	0.79	49.6	82.6	0.57	1.65
				0.5%	-0.06	1.28	45.6	82.2	0.70	2.20
18	Hill	58	CVaR	2.5%	-2.53	11.70	25.3	67.5	3.94	8.47
				1%	-4.60	14.20	24.2	74.6	5.26	16.39
				0.5%	-7.82	24.82	25.9	78.5	6.79	28.02
			CES	2.5%	-6.88	20.00	63.8	76.1	13.74	23.84
				1%	-12.91	26.17	59.4	79.8	21.82	47.51
				0.5%	-19.77	46.54	52.9	80.5	31.93	77.41
	MR	62	CVaR	2.5%	-1.29	11.00	84.2	63.7	16.30	9.09
				1%	-2.00	12.30	88.4	67.8	25.14	15.01
				0.5%	-3.66	21.67	87.2	68.7	35.86	23.27
			CES	2.5%	-3.37	17.2	82.1	72.0	24.72	19.45
				1%	-6.50	20.64	84.5	76.3	38.37	35.20
				0.5%	-10.64	38.57	83.6	75.7	55.50	55.22
19	Hill	57	CVaR	2.5%	0.00	1.78	25.7	73.6	1.14	2.86
				1%	-0.22	2.24	26.9	82.6	1.45	4.84
				0.5%	-0.80	2.93	32.4	89.5	1.72	8.06
			CES	2.5%	-0.69	2.60	66.9	87.5	3.21	6.46
				1%	-1.75	3.93	58.9	90.5	4.75	11.39
				0.5%	-3.16	5.79	48.8	91.0	6.32	17.87
	MR	67	CVaR	2.5%	0.59	1.72	82.3	65.6	4.23	83.02
				1%	0.75	2.18	84.3	70.9	6.22	4.70
				0.5%	0.57	2.55	88.4	77.7	8.27	6.96
			CES	2.5%	0.45	2.18	82.9	78.9	5.67	5.64
				1%	0.00	3.06	85.8	85.2	8.30	9.33
				0.5%	-0.75	4.27	88.5	87.1	11.13	13.74

The table shows in the columns the average of $k*$, bias RMSE, coverage probabilities in %, and average interval lengths for the Hill and MR estimator respectively. For simulation models 18 and 19, the results are multiplied by 10^3.